ELSEVIER

International Journal of Heat and Fluid Flow 23 (2002) 744–749

International Journal of HEAT AND FLUID FLOW

www.elsevier.com/locate/ijhff

Vortex generating jets; effects of jet-hole inlet geometry

James P. Johnston [a,*], Bruce P. Mosier [b], Zia U. Khan [c]

[a] *Department of Mechanical Engineering, Stanford University, Stanford, CA 94305-3030, USA*
[b] *Sandia National Labs, 7011 East Ave., MS 9951, Livermore, CA 94550, USA*
[c] *A.T. Kearney, 153 East 53rd Street, New York, NY 10022, USA*

Received 14 September 2001; accepted 8 January 2002

Abstract

An experimental study of flow downstream of round, pitched and skewed wall-jets (vortex generating jets) is presented to illustrate the effects of changing the geometric inlet conditions of the jet-holes. In one case the jet-hole has a smoothly contoured inlet, and in the other the inlet was a sharp-edged, sudden contraction. The test region geometry, mean jet flow and cross-flow conditions were otherwise identical. In both cases, dominant streamwise vortex structures are seen in the boundary layer downstream; the flow and turbulence is nearly the same in the far-field starting downstream of $x/D = 5$. In the near-field, for $x/D < 5$, there are significant differences; turbulence levels are higher, and the start of the dominant vortex shape is less clear for the sharp-edged case. This is believed to be the result of flow separation and free shear layer instability inside the jet-hole which are not present for the smoothly contoured case.

1. Introduction

Vortex-generating wall jets may be used (i) to mix low-momentum boundary-layer fluid with high-momentum freestream fluid for the suppression of flow separation (Johnston and Nishi, 1990), or (ii) for film cooling of gas turbine blades using cross-compound injection of compressor bleed air (Honami et al., 1994; Gartshore et al., 2001). However, modification of geometry at the inlet to the short jet-hole may have substantial effects on mean flow and turbulence development downstream of jet injection; effects that may be important in both applications.

Vortex generating jets (VGJs) introduced through holes in a wall into a cross-flow (main flow in axial direction, see Fig. 1, Khan and Johnston, 2000) with various velocity ratios (jet speed/cross-flow speed) have been studied experimentally at several downstream planes. A short jet-hole was pitched up from the wall at 30°, and skewed relative to the cross-flow direction (x-axis) by 60°. Detailed measurements of mean velocity, mean streamwise vorticity, and the six Reynold's stresses were obtained with a three-component laser-Doppler velocimetry (LDV).

Here, two different, round jet-hole configurations were employed (see Fig. 1). Both had identical diameters, $D = 25.4$ mm and lengths, $L = 88.4$ mm. The flow fields that result from the jet-hole with the *smoothly contoured* inlet nozzle were described in the earlier work. This configuration created a flow in the jet-hole which was steady and distorted, but smoothly varying, across the hole's exit plane, and it filled the hole without separation. In the second configuration, flow entered the *sharp-edged* hole at very low speed from a large plenum chamber, and at the hole's entrance it separated on the sharp edge to form a recirculating region on the downstream side of the hole. The resulting changes in mean velocity profile and turbulence in the jet flow which emerges from the sharp-edged hole into the cross-flow were expected to change the flow structure downstream, in particular the dominant streamwise vortex, but the extent of the changes and the degree of the effects that would occur were unknown.

Compton and Johnston (1992) and Khan and Johnston (1999) using smoothly contoured jet-holes showed that a skew of 60° appeared to maximize the strength of the dominant vortex. With this in mind, 60° was chosen for the sharp-edged hole, a geometry more likely to be

* Corresponding author. Fax: +1-650-723-4548.
E-mail address: jpj@stanford.edu (J.P. Johnston).

0142-727X/02/$ - see front matter © 2002 Elsevier Science Inc. All rights reserved.
PII: S0142-727X(02)00138-8

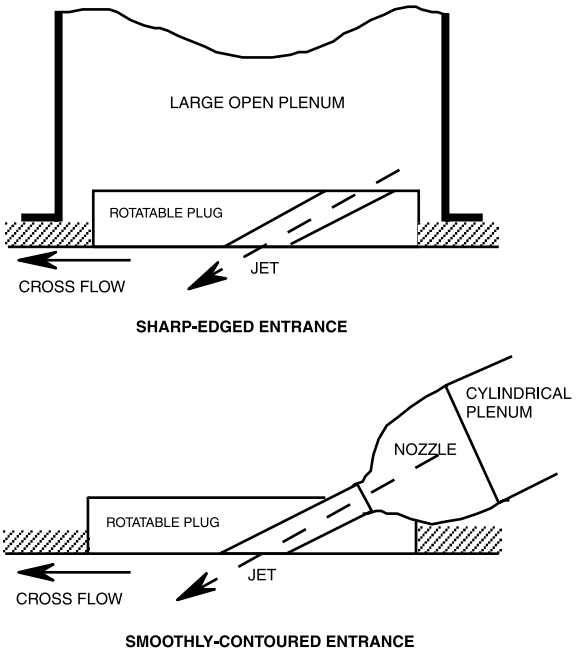

Fig. 1. Two jet-hole configurations (see Fig. 2 in Khan and Johnston (2000) for more detail). The pitch angle of the holes was 30° from the plane of the wall and the jet-hole was skewed at 60° from the downstream direction of the cross-flow. Hole: diameter, $D = 25.4$ mm; length, $L = 88.4$ mm.

used in practice than the complex smoothly contoured geometry.

The choice of hole length ($L/D = 3.5$) was based on an estimate of what might be used in a typical VGJ application. The holes must be long enough to guide the jet at the desired angle, but not too long to cause large pressure losses. In addition, the Reynolds number of the flow in the jet-hole (about 5000 based on diameter) was chosen to match conditions of some VGJ applications. These geometries and flow conditions also overlap with some film cooling cases, and thus should provide both qualitative design information and several sets of detailed data that may be useful as comparative results for the development of CFD codes (see Gartshore et al., 2001).

2. Experimental procedure

The experiments were conducted in a low-speed, U-shaped, free-surface water channel with a single jet-hole plug inserted near the spanwise center of a vertical flat wall on which a two-dimensional boundary layer grew. The *cross-flow* and the *mean jet* speeds (U_e and V_{jet}) were both set at 20 cm/s for the quantitative, LDV measurements, and both were 5 cm/s for flow visualization. The velocity ratio $VR = V_{jet}/U_e = 1$ in all cases.

The single jet-hole was located on the test wall at a spanwise (z) distance 10 D below the free surface and 13 D above the channel bottom. In the measurement region ($x/D = 0$ to 20, $y/D = 0$ to 3, $z/D = -3$ to $+5$) neither the bottom of the channel nor the free surface substantially affected the results. The same may be stated of the other vertical wall of the channel located at $y = 15$ D opposite the test wall.

The LDV measurements were made using a three-component LDV system that was composed of one two-component probe and one single-component probe. The probes were orthogonal to each other with intersecting measuring volumes. Using the side scatter from the seed particles, each probe employed the other probe's receiving optics. This guaranteed that the measuring volumes from the two probes were coincident for all of the measurements. The measuring volume was nearly spherical and approximately 2 viscous lengths in diameter. The method is described in detail by Khan and Johnston (1999) where a detailed error analysis is presented in Appendix B. The uncertainties (95% confidence) of the mean velocity components are $\pm 0.005 U_e$ and for turbulence kinetic energy, $\pm 0.01 U_e^2$.

LDV data were taken in planes perpendicular to the wall at $x/D = 5$, 10, and 20. x/D is the distance, in jet-hole diameters, downstream of the center of the jet-hole at its exit, where it intersects the test surface (wall). y/D profiles, numbering 14 points from near the wall to the freestream, were obtained at 20 to 21 spanwise locations for each data plane. With the jet flow off, the test surface boundary layer was two-dimensional and turbulent, with a momentum thickness Reynolds number of 1100 and a physical thickness of about 2D. In the results, it is seen that the jet flow severely perturbs the spanwise two-dimensionality creating what has been called a dominant vortex downstream. Velocity components and Reynolds stresses are made dimensionless using the cross-flow free stream speed U_e.

Flow visualization, using Fluorescein dye dissolved in water, was performed in the same manner as described in Khan and Johnston (1999). The dyed fluid was mixed into the jet fluid in the plenum region, well upstream of the inlet to the jet-hole. No boundary layer trip was used, and cross-flow wall was shortened. Thus, with $U_e = 5$ cm/s, a thin, laminar boundary layer was present at the location of the jet-hole. The lower flow speeds and elimination of the thicker, turbulent boundary layer on the test surface improved the quality of the flow visualization although the flow conditions no longer matched those of typical VGJ or film cooling applications as well as the LDV results. Video images, oriented perpendicular to the cross-flow (x-axis), were acquired at several planes where an argon-ion laser sheet was passed into the flow to excite fluorescence in the dye.

3. Experimental results

Flow visualization of the jet fluid for both the sharp-edge inlet and for the smoothly contoured inlet, at

various downstream positions near the center of the jet-hole, were included in video studies of the near-field. Two video frames for both cases are shown in Fig. 2. In all four images, the test wall is in the top 1/4 of the photo where the fluorescing dye in the jet fluid is reflected. A yellow line indicates the approximate location of the wall. The jet penetrates the wall from upper right to lower left just upstream of the light plane and the approximate location and orientation of the jet is shown by the red arrow superimposed on each picture.

For the *smoothly contoured* case, the flow appeared steady and the two views illustrate the early development of the dominant vortex on the right hand side of the dyed jet fluid. It is larger and slightly more chaotic downstream at $x/D = 2.0$ than at 0.72. The smaller vortex to the left resulted from the interaction of the cross-flow's wall boundary layer as it meets the blockage presented by the skewed jet.

The flow is very unsteady in the *sharp-edge* case, and thus no individual video fame is truly representative. Although the Reynolds number is low, the very chaotic motions seen in the video will be called turbulence. The overall flow structure of the sharp-edge jet is similar to that of the smooth-inlet jet in that both appear to contain a dominant vortex (right hand side of each frame). The general circulation associated with the dominant vortex is not clear in single frames, but may be more easily discerned by watching the video. In contrast to the smoothly contoured case where the flow is relatively steady, there is substantially more chaotic unsteadiness in the sharp-edge case. It is likely that the origin of this enhanced unsteadiness lies inside the jet-hole. The flow separates at the sharp edge as it enters the jet-hole and creates a free shear layer downstream. We believe that the Kelvin–Helmholtz instability of this free shear layer enhances the unsteadiness of the flow in the jet and is the main source of the turbulence in the near-field ($x/D < 5$) which is not seen in the smoothly contoured case. Note that some turbulence does develop in the near-field for the smoothly contoured case at higher jet speeds where K–H roll-ups tend to be seen on the top of the skewed jet, just above the hole, as it turns downstream.

Quantitative mean velocity data are compared side-by-side in Figs. 3 and 4. They show the general circulation patterns of the dominant vortex in the far-field, at $x/D = 10$ and 20. The circulation in the y–z plane (secondary flow) is indicated by the $V + W$ vectors which are overlaid on the U coutour lines. Close to the jet-hole, at $x/D = 5$, the clear existence of a well-developed vortex core is questionable, especially for the sharp-edged

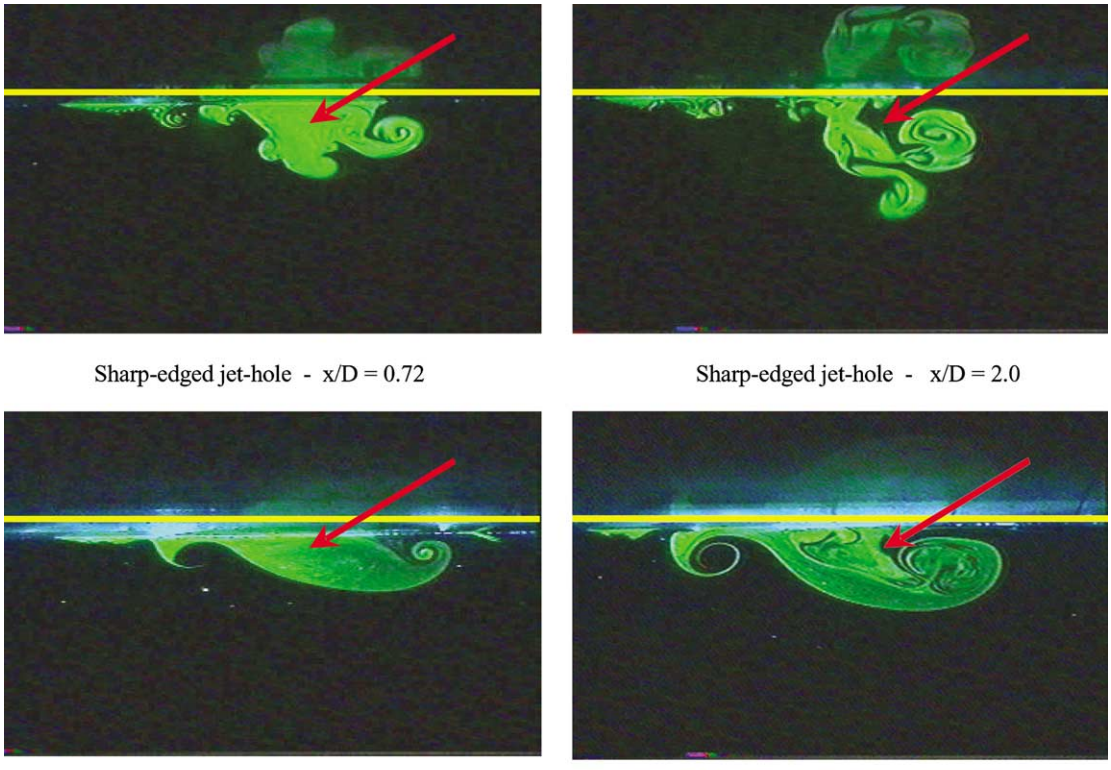

Fig. 2. Jet structure in dyed jet fluid illuminated normal to cross-flow by thin plane of laser light at two positions in the near-field, downstream of the center of the exit of the jet-hole. The reflection of the image in the smooth wall is seen at the top of each photo. The yellow line shows as test surface wall. Location of the jet indicated by the red arrow. Jet-hole pitch = 30°, skew = 60°, and $U_e/V_{jet} = 1.0$ (jet speed and freestream speed of 5 cm/sec).

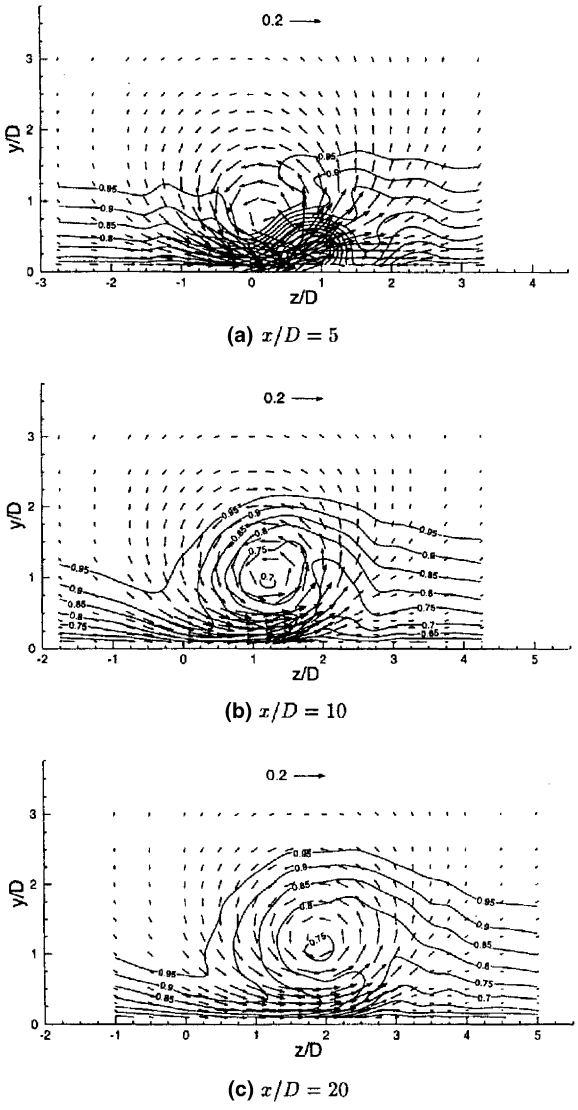

Fig. 3. *Sharp-edge jet-hole*—Contours of mean streamwise velocity, U, with secondary flow ($V + W$) vectors superposed at three downstream stations. Outer contour is set at $U/U_e = 0.95$, central contour = 0.7 for $x/D = 10$ but at 0.75 for $x/D = 20$. Secondary vector of 0.2 U_e shown for reference.

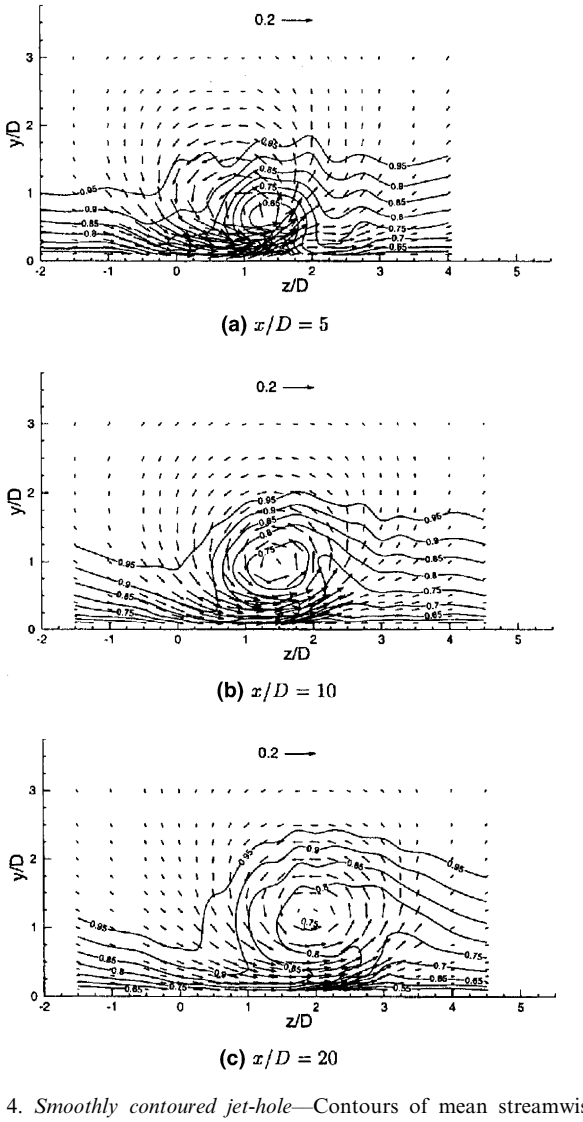

Fig. 4. *Smoothly contoured jet-hole*—Contours of mean streamwise velocity, U, with secondary flow ($V + W$) vectors superposed at three downstream stations. Outer contour is set at $U/U_e = 0.95$, central contour = 0.8 for $x/D = 5$ but at 0.75 for $x/D = 10$ and 20. Secondary vector of $0.2U_e$ shown for reference.

case. Further downstream, at $x/D = 10$ and 20, the low speed, wall boundary layer eventually ends up in the core region as evidenced by the low values of streamwise velocity ($U = 0.75$) on closed contours close to the center of secondary circulation.

These observations were augmented by study of contours of mean streamwise vorticity (computed from the mean secondary velocities, V and W). Here, a region that might be called the core of the dominant vortex is seen at $x/D = 5$, but the contour lines outside the core are not the circular to oval shapes expected for the true vortex flow, especially in the sharp-edged case. Table 1 shows the peak magnitude of vorticity in the core region at $x/D = 5$, 10, and 20. The rate of decay of streamwise vorticity with downstream distance is strongest upstream of $x/D = 10$ for the sharp-edged jet-hole, but about the same for both cases downstream of $x/D = 10$, in the far-field.

Comparison of the secondary flow vectors in Figs. 3a and 4a indicates that the dominant vortex is stronger in the sharp-edge case, an observation supported by higher values of core vorticity (Table 1). These observations

Table 1
Magnitude of mean streamwise vorticity in the dominant vortex core for two jet-hole inlet shapes

x/D	Sharp-edge	Smooth-contour
5.0	2.79	1.60
10.0	0.97	0.90
20.0	0.57	0.45

may be explained if the flow in the jet-hole is partially blocked by reverse flow due to separation over the sharp-edge as the flow enters the jet-hole. Such a blockage (effective area reduction) would cause the actual jet speed to be somewhat higher than the nominal mean value of 20 cm/s which was forced by control of the flow rate into the jet-hole. The result is that the effective velocity ratio, VR, for the sharp-edged case is higher than 1.0, the nominal value. It has been shown, Compton and Johnston (1992), that a higher VR value creates a stronger dominant vortex with a larger core streamwise vorticity in the far field ($x/D = 10$ and 20 in our flows).

Quantitative data for the turbulent kinetic energy (actually, $q^2 = 2$ K) at $x/D = 5$, 10, and 20 are shown side-by-side in Figs. 5 (sharp-edged) and 6 (smoothly contoured). The vectors represent the transport of q^2 by the turbulence in the plane of data. For details on the transport of q^2 refer to discussion in Khan and Johnston (2000). The most interesting feature of these results is seen when the cases are compared at $x/D = 5$, the downstream end of the near-field. The jet-hole with the sharp-edged inlet produced almost double the turbulent kinetic energy as the smoothly contoured case. However, at the downstream stations ($x/D = 10$ and 20), the turbulence is only slightly higher for the sharp-edged case. This is also illustrated in Table 2. In the far-field, the initial rate of decay of turbulence in the case of the sharp-edged hole is higher but it falls to nominal values downstream.

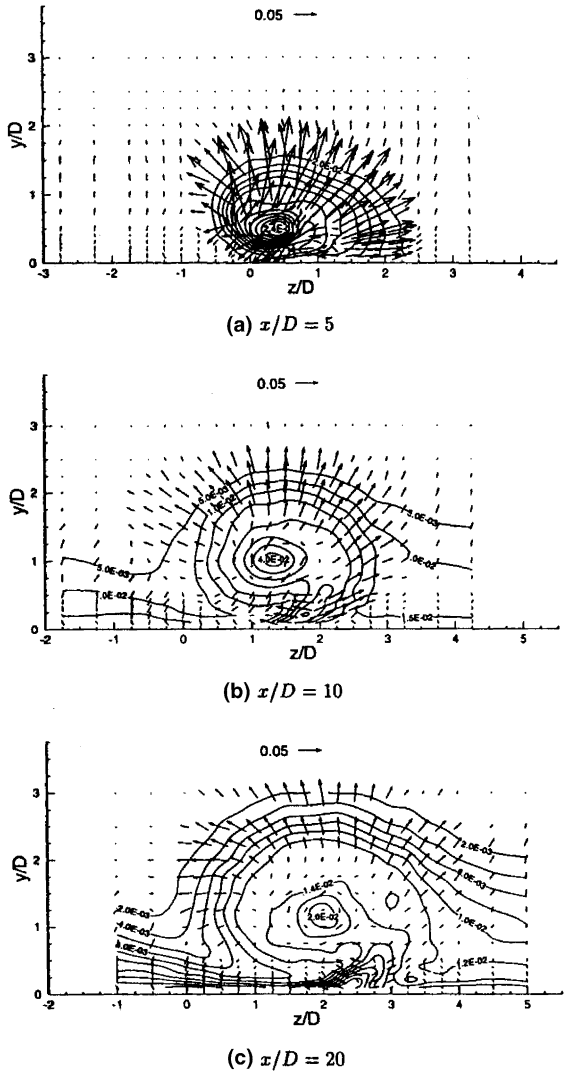

Fig. 5. *Sharp-edge jet-hole*—Contours of q^2 ($2 \times$ turbulent kinetic energy) normalized on U_e^2. Vectors represent transport of q^2 by turbulence velocity (V and W) in y–z plane. Max/min contour values are 0.24/0.02 at $x/D = 5$; 0.04/0.005 at $x/D = 10$; 0.02/0.002 at $x/D = 20$.

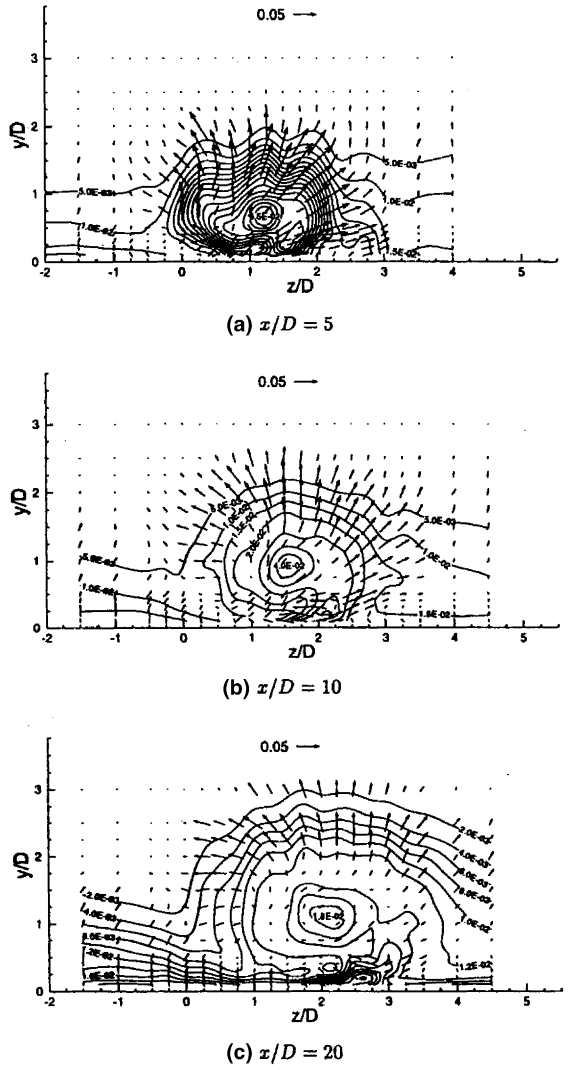

Fig. 6. *Smoothly contoured jet-hole*—Contours of q^2 ($2 \times$ turbulent kinetic energy) normalized on U_e^2. Vectors represent transport of q^2 by turbulence velocity (V and W) in y–z plane. Max/min contour values are 0.085/0.005 at $x/D = 5$; 0.04/0.005 at $x/D = 10$; 0.02/0.0018 at $x/D = 20$.

Table 2
q^2 ($2 \times$ turbulence kinetic energy) in the dominant vortex core for two jet-hole inlet shapes

x/D	Sharp-edge	Smooth-contour
5.0	0.240	0.085
10.0	0.040	0.040
20.0	0.020	0.018

The high, initial turbulence level is thought to originate in the instability and unsteadiness of the shear-layer over the recirculation region formed by separation at the inlet to the sharp-edged jet-hole (see discussion in flow visualization, above). Intense shear-layer turbulence occurs on a smaller scale and at higher frequency than the turbulence generated later due to the jet/cross-flow interaction outside of the hole. This observation may help explain its rapid initial rate of downstream decay.

4. Conclusions

Near field region, $x/D \leqslant 5$. Flow visualization and LDV data of the resulting jet structure showed that the change of the jet inlet geometry had substantial effects. Sharp edges over which inlet flow can separate create a stalled region inside the hole. Area blockage by the low-speed stalled region effectively narrows and accelerates the jet core flow so that it is faster than the mean jet speed (based on hole cross sectional area). A thin shear layer exists along the edge of the separated jet, inside the hole. This shear layer is unstable and its unsteadiness is believed to be the source of intense turbulence not observed in the near field of the smoothly contoured case where no flow separation occurs inside the jet-hole. The additional turbulence and dissipation generated as a result of local flow separation over the sharp-edged inlet and the blockage effect due to the recirculating region inside the hole had substantial consequences, the most important being a more rapid initial dissipation of the stronger dominant vortex for the sharp-edge case.

Far field region, $x/D > 10$. Eventually, far downstream of the jet-hole, the effects of initial conditions damp out and the strength and decay rate of the dominant streamwise vortex depends only on gross hole geometry: pitch and skew angle, and the ratio of mean jet speed to cross-flow speed. The measured velocity, streamwise vorticity, and turbulence statistics in the far-field region, at $x/D = 10$ and 20, were nearly identical for both inlets.

The possible consequences of these results are different, depending on the application. In the case of VGJs for separation control the use of a smoothly contoured inlet would appear to have little value because the strength of the dominant vortex, the principle cross-stream mixing mechanism is unchanged in the far-field. On the other hand, for film cooling with cross-compound injection, the higher turbulence levels in the region near the hole in the case of the sharp-edged hole might increase local heat transfer rates and decrease cooling effectiveness. This points to a potential benefit if smoothly contoured film cooling holes could be used in applications where the jet-hole length is short.

References

Compton, D.A., Johnston, J.P., 1992. Streamwise vortex production by pitched and skewed jets in a turbulent boundary layer. AIAA Journal 30, 640–647.

Gartshore, I., Salcudean, M., Hassan, I., 2001. Film cooling injection hole geometry: hole shape comparison for compound cooling orientation. AIAA Journal 39, 1493–1499.

Honami, S., Shizawa, T., Uchiyama, A., 1994. Behavior of the laterally injected jet in film cooling: measurements of surface temperature and velocity/temperature field within the jet. ASME Journal of Turbomachinery 116, 106–112.

Johnston, J.P., Nishi, M., 1990. Vortex generator jets—means for flow separation control. AIAA Journal 28, 429–436.

Khan, Z.U., Johnston, J.P., 1999. On the dominant vortex created by a pitched and skewed jet in crossflow. Report TSD-122, Mechanical Engineering Division, Stanford University, March 1999.

Khan, Z.U., Johnston, J.P., 2000. On Vortex generating jets. International Journal of Heat and Fluid flow 21, 506–511.